β-Substituted cyclohexanecarboxamide cathepsin K inhibitors: Modification of the 1,2-disubstituted aromatic core

Joël Robichaud,[a],* Christopher I. Bayly,[a] W. Cameron Black,[a] Sylvie Desmarais,[a] Serge Léger,[a] Frédéric Massé,[a] Daniel J. McKay,[a] Renata M. Oballa,[a] Julie Pâquet,[a] M. David Percival,[a] Jean-François Truchon,[a] Gregg Wesolowski[b] and Sheldon N. Crane[a]

[a]Merck Frosst Centre for Therapeutic Research, 16711 TransCanada Highway, Kirkland, Que., Canada H9H 3L1
[b]Merck Research Laboratories, West Point, PA 19486, USA

Abstract—Further SAR study around the central 1,2-disubstituted phenyl of the previously disclosed Cat K inhibitor (−)-**1** has demonstrated that the solvent exposed P2–P3 linker can be replaced by various 5- or 6-membered heteroaromatic rings. While some potency loss was observed in the 6-membered heteroaromatic series (IC_{50} = 1 nM for pyridine-linked **4** vs 0.5 nM for phenyl-linked (±)-**1**), several inhibitors showed a significantly decreased shift in the bone resorption functional assay (10-fold for pyridine **4** vs 53-fold for (−)-**1**). Though this shift was not reduced in the 5-membered heteroaromatic series, potency against Cat K was significantly improved for thiazole **9** (IC_{50} = 0.2 nM) as was the pharmacokinetic profile of *N*-methyl pyrazole **10** over our lead compound (−)-**1**.
© 2007 Elsevier Ltd. All rights reserved.

Bone tissue remodeling is a dynamic process involving multiple biological pathways wherein bone resorption is mediated by highly specialized cells called osteoclasts. After tightly binding to the bone surface, these osteoclasts create an acidic lacuna into which the lysosomal cysteine protease cathepsin K (Cat K) is secreted and effects cleavage of type I collagen (i.e., the main protein constituent of bone).[1] The elucidation of this biological mechanism has rendered it an attractive target for the development of new anti-resorptive therapies for bone diseases such as osteoporosis.[2]
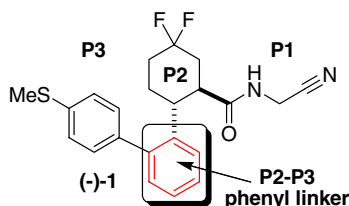

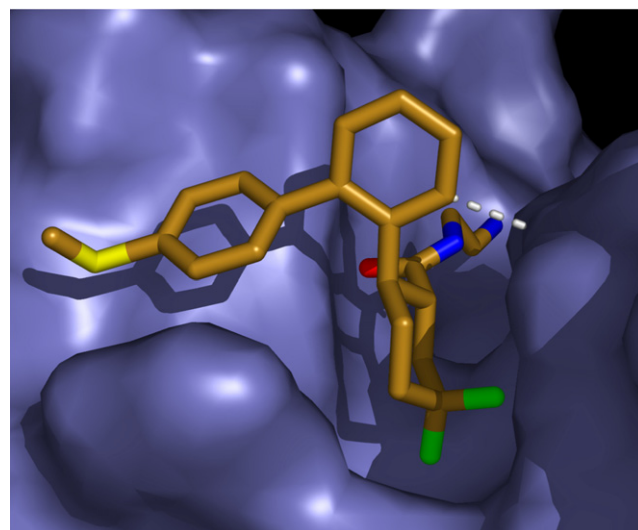**Figure 1.** Exploring the SAR around the 1,2-disubstituted P2–P3 linker.

Figure 2. The average structure resulting from 100 ps MD studies of (−)-**1**in Cat K is shown. The P2–P3 phenyl linker is solvent exposed, while P2 goes deeply in the S2 pocket and P3 forms lipophilic interactions. Dashed line shows a steric contact between ligand and active site.

Our ongoing research in this field has already led to the disclosure of SAR for several series of Cat K inhibitors bearing a P2 leucine side chain.[3] We recently reported a
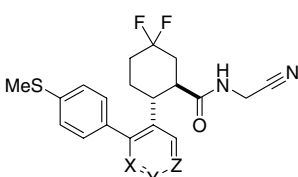
new, structurally distinct series wherein this P2 leucine side chain was replaced with a β-substituted cyclohexyl moiety (see Fig. 1).[4] These efforts led to the identification of the potent and selective inhibitor (−)-1 possessing a 1,2-disubstituted phenyl linking the P2–P3 portion of the molecule. The P3 SAR was found to be different from other nitrile warhead based inhibitors in that a basic group in P3 was not required for sub-nanomolar potency, but rather a thiomethyl ether in P3 was preferred. In addition, the *gem*-difluoro substitution of the cyclohexyl in P2 was found to be critical to achieve a good pharmacokinetic profile.
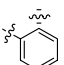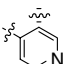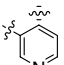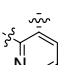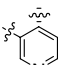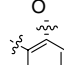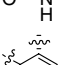
We now report further SAR based on inhibitor (−)-1 where the 1,2-disubstituted phenyl ring is replaced with 5- and 6-membered heteroaromatic rings. Part of our strategy was to reduce the >50-fold loss of potency of (−)-1 in the functional bone resorption assay as compared to the enzyme assay.[4] We reasoned that our inhibitors' high lipophilic nature might be partly responsible for this shift. Since modeling studies demonstrated that

the P2–P3 aromatic linker is solvent-exposed (see Fig. 2), we surmised that the introduction of polarity in this region would be tolerated and that modifications around this core might succeed in reducing the observed shift.

We began our SAR in the 6-membered heteroaromatic rings (see Table 1) by synthesizing the three isomeric pyridines **2**, **3**, and **4**. The 3- and 4-pyridyl substituted compounds **3** and **4** showed slight erosion in potency against Cat K (IC$_{50}$ = 1 nM) while maintaining an excellent selectivity profile against other cathepsins. More important, however, is the fact that pyridines **3** and **4** showed a significant decrease in the observed shift (18- and 10-fold, respectively) in the bone resorption functional assay. The 3-pyridyl *N*-oxide **5** afforded a significant loss in potency (IC$_{50}$ = 5 nM) without maintaining the improved shift in the functional assay (15-fold). The two isomeric pyridones **6** and **7** displayed profiles similar to that of the pyridine *N*-oxide **5** (IC$_{50}$ = 8 and 4 nM, respectively) where the shift in the bone resorption

Table 1. Inhibition of Cat K with 6-membered heteroaromatic compounds

Ar	Compound[a]	hrab Cat K IC$_{50}$[b] (nM)	rab Cat K IC$_{50}$[b] (nM)	Cat L[c]/CatK	CatB[c]/CatK	Cat S[c]/CatK	Bone res IC$_{50}$[d] (nM)	Shift (fold)[e]
	(−)-**1**	0.3	0.3	780	>36,000	940	16	53
	(±)-**1**	0.5	0.5	880	>120,000	1100	38	76
	2[f]	2	2	260	>5000	450	58	29
	3	1	1	520	>10,000	720	18	18
	4	1	1	540	>10,000	850	10	10
	5	5	5	460	>2000	480	75	15
	6	8	6	430	>1250	310	84	14
	7	4	5	410	1200	540	20	4

[a] All compounds in the 5- and 6-membered heteroaromatic series were synthesized and evaluated as racemic mixtures.
[b] IC$_{50}$ values represent an average of at least n = 2 and variation was within 2-fold. Humanized rabbit (hrab) Cat K was utilized, see Ref. 5 for conditions.
[c] Human enzyme was used for these assays, see Ref. 6 for conditions.
[d] See Ref. 6 for assay conditions.
[e] Shift is calculated by dividing the potency obtained in the bone resorption assay over the potency observed in the enzyme assay using rab Cat K.
[f] Pyridine **2** contains a CFH$_2$ group in P3 instead of a CH$_3$ on the sulfur atom.

assay (14- and 4-fold, respectively) was likewise reduced in comparison with biaryl (−)-**1**. These results support our hypothesis that the high lipophilic character of inhibitors such as (−)-**1** has a negative impact on the shift observed in the functional assay.
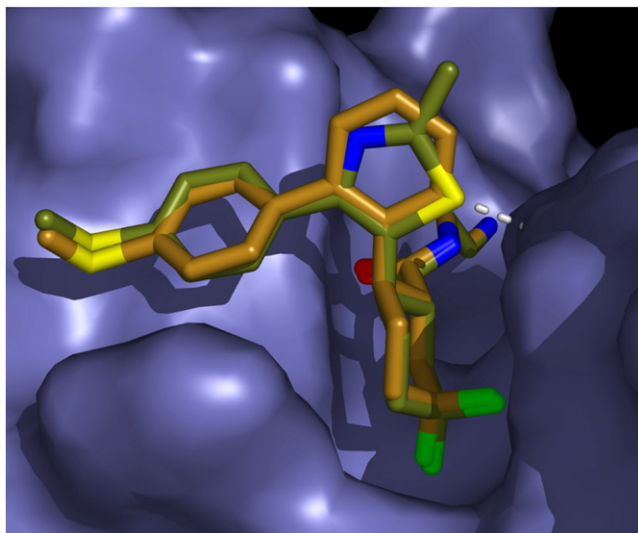

Figure 3. Superposition of average structures from 100 ps MD trajectories of compound (−)-**1** with compound **9** in the Cat K active site. The dashed line shows steric contact between compound **9** and the active site. Overall **9** sits just over 0.3 Å deeper into the active site.

The pharmacokinetic profile in rats (PO: 5 mg/kg, IV: 1 mg/kg) of the 3-pyridyl analog **3** was assessed (F = 65%, $T_{1/2}$ = 1.0 h, AUC = 8.6 μM h) but was found to be somewhat inferior to that of the biaryl analog (−)-**1** (F = 39%, $T_{1/2}$ = 3.5 h, AUC = 18.5 μM h).

While all of the compounds generated in the 6-membered heteroaromatic linked series succeeded in decreasing the observed shift in the functional bone resorption assay, none of them were as potent as (±)-**1**. Molecular dynamics calculations suggested that the replacement of the 6-membered heteroaromatic linker with a 5-membered ring would reduce steric contact of the inhibitor with the side of the S2 pocket (dashed line in Figs. 2 and 3), while increasing the angle of the bond vector reaching towards S3, thereby also reducing the steric interaction between the SMe group and the S3 pocket. In addition, the dihedral angle between the 5-membered heteroaromatic ring and the phenyl ring in P3 is smaller than the corresponding dihedral angle in (−)-**1**. The net effect of these changes would be to allow the inhibitors to sit closer to the surface of the enzyme and thereby enhance their potency.

In line with this rationale, the central 1,2-disubstituted phenyl ring of (±)-**1** (see Table 2) was replaced with a 5-membered benzyl-substituted triazole to afford compound **8**. And while inhibitor **8** again showed very little shift in the functional assay (4-fold), there was a 10-fold loss in potency in the enzymatic assay (IC$_{50}$ = 2 nM). Hypothesizing that the bulky benzyl group was

Table 2. Inhibition of Cat K with 5-membered heteroaromatic compounds

Ar	Compound[a]	hrab Cat K IC$_{50}$[b] (nM)	hrab Cat K IC$_{50}$[b] (nM)	Cat L[c]/CatK	Cat B[c]/CatK	Cat S[c]/CatK	Bone Res IC$_{50}$[d] (nM)	Shift (fold)[e]
phenyl	(−)-**1**	0.3	0.3	780	>36,000	940	16	53
	(±)-**1**	0.5	0.5	880	>120,000	1100	38	76
triazole BnN-N	**8**	2	9	350	1 400	180	33	4
thiazole N=	**9**	0.2	0.1	270	14 990	380	17	170
pyrazole N-N	**10**	0.4	0.4	730	9 500	490	41	103

[a] All compounds 5- and 6-membered heteroaromatic series were synthesized and evaluated as racemic mixtures.

[b] IC$_{50}$ values represent an average of at least n = 2 and variation was within 2-fold. Humanized rabbit (hrab) Cat K was utilized, see Ref. 5 for conditions.

[c] Human enzyme was used for these assays, see Ref. 6 for assay conditions.

[d] See Ref. 6 for assay conditions.

[e] Shift is calculated by dividing the potency obtained in the bone resorption assay over the potency observed in the enzyme assay using rab Cat K.

detrimental to the potency of **8**, debenzylation was attempted under standard conditions but failed to provide us with the debenzylated triazole.

The 2-methyl thiazole **9** was prepared and succeeded in achieving sub-nanomolar potency against Cat K ($IC_{50} = 0.2$ nM), being even more potent than our lead compound (±)-**1** ($IC_{50} = 0.5$ nM). This result lent support to our modeling hypothesis. On the other hand, the observed shift in the functional assay for inhibitor **9** worsened (170-fold) and so did the selectivity profile of **9** against other cathepsins. While the *N*-methyl-substituted pyrazole **10** again displayed sub-nanomolar potency against Cat K ($IC_{50} = 0.4$ nM) along with an improved selectivity profile against Cat L and S, the shift in the functional assay remained high (103-fold).

We surmise that the lack of improvement in the functional assay shift with these 5-membered heteroaromatic inhibitors is due to their high lipophilicity in comparison with the pyridine/pyridone compounds. In contrast, however, with the 6-membered heteroaromatic series, the pharmacokinetic profile in rats (PO: 10 mg/kg, IV: 5 mg/kg) of the *N*-methyl pyrazole analog **10** ($F = 100\%$, $T_{1/2} = 4.6$ h, AUC = 28.9 μM h) was found to be superior to that of our lead compound (−)-**1** ($F = 39\%$, $T_{1/2} = 3.5$ h, AUC = 18.5 μM h).
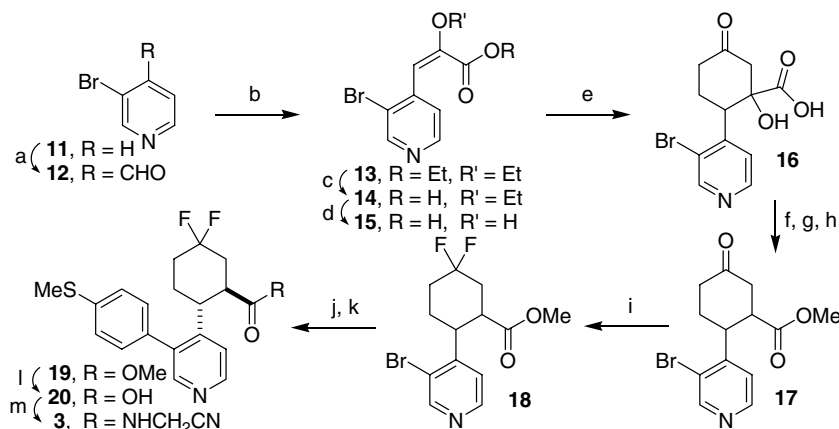
Given that the SAR modifications all centered on the core of the inhibitors, each new heterocyclic compound had to be synthesized in a separate fashion. Two general strategies were employed to synthesize these inhibitors. The first utilized a Diels–Alder approach (for the synthesis of thiazole **9** and pyrazole **10**). The second employed a base-catalyzed addition of methyl vinyl ketone onto a properly functionalized pyruvic acid derivative which underwent concomitant intramolecular cyclization to afford the cyclohexane-substituted heteroaromatic core (this approach was utilized for the

synthesis of triazole **8**, pyridines **2**, **3**, and **4**, pyridine *N*-oxide **5**, and pyridones **6** and **7**).
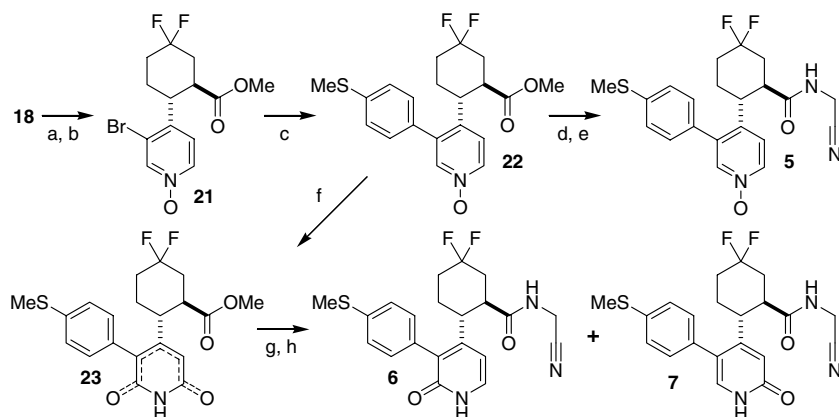
The synthesis of the 3-pyridyl analog **3** began with commercially available 3-bromopyridine **11** which was deprotonated with LDA and quenched with DMF to afford aldehyde **12** (see Scheme 1). Wittig reaction with Et_3N as base afforded the key pyruvate ester **13** which was hydrolyzed to the corresponding pyruvate acid **15** in two steps. Treatment of **15** with methyl vinyl ketone under basic conditions yielded **16** via a Robinson annulation type reaction. Alcohol elimination under acidic conditions provided the α,β-unsaturated enone which was then reduced with activated zinc dust to ketone **17** (predominantly as the cis isomer). Difluorination of the ketone **17** with DAST yielded the desired difluoro analog **18**,[7] which was cross-coupled with 4-(methylthio)benzeneboronic acid and equilibrated to the more thermodynamically stable trans isomer **19** under basic conditions. Hydrolysis of the ester **19** followed by coupling with aminoacetonitrile provided the final compound **3**.

The sequence leading to the pyridine *N*-oxide **5** and the corresponding pyridones **6** and **7** began with the equilibration of **18** under basic conditions followed by N-oxidation with *m*-CPBA to afford compound **21** (see Scheme 2). The usual sequence involving Suzuki cross-coupling, hydrolysis, and amide coupling then afforded *N*-oxide **5**. Treatment of **22** with trifluoroacetic anhydride afforded a mixture of two isomeric pyridones (**23**) which were hydrolyzed and coupled as above to afford the two isomeric pyridones **6** and **7** after separation by flash chromatography.
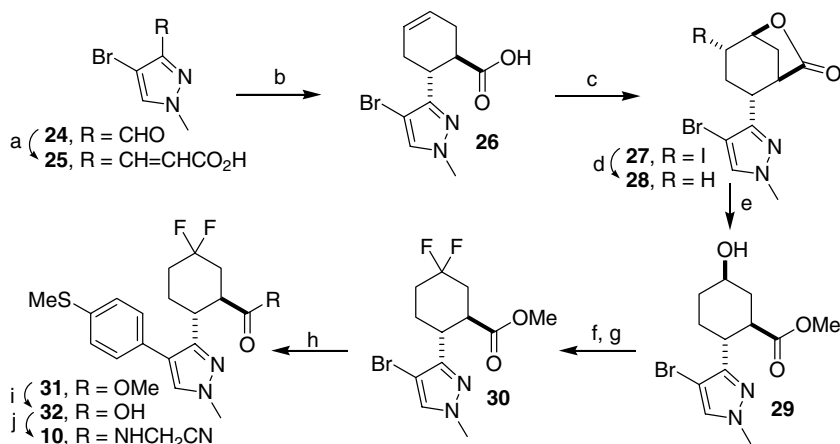
The synthesis of pyrazole **10** (see Scheme 3) began with the commercially available aldehyde **24** which was converted to the α,β-conjugated carboxylic acid **25** via a Knoevenagel condensation. The Diels–Alder reaction of **25** with butadiene in a stainless steel bomb at

Scheme 1. Synthesis of the pyridine analog **3**. Reagents and conditions: (a) *n*-BuLi, *i*-Pr$_2$NH, THF, then DMF, −78 °C → rt, 1.5 h, 45%; (b) Ph$_3$P=C(OEt)CO$_2$Et, CHCl$_3$, 18 h, 90%; (c) NaOH, MeOH, rt, 18 h; (d) HCl, 1,4-dioxane, 110 °C, 1.5 h, 46% (two steps); (e) methyl vinyl ketone, MeOH, NaOH, 0 °C → rt, 2 h, 56%; (f) H$_2$SO$_4$, H$_2$O, 60 °C, 18 h, 96%; (g) Zn*, AcOH/Py/H$_2$O (6:3:1), rt, 1 h, 74%; (h) CH$_2$N$_2$, Et$_2$O, 100%; (i) DAST, TsOH, CH$_2$Cl$_2$, rt → 40 °C, 18 h, 58% (traces of alkenes); (j) 4-(methylthio)benzeneboronic acid, PdCl$_2$(dppf)·CH$_2$Cl$_2$, aq 2 M Na$_2$CO$_3$, DMF, 90 °C, 18 h, 56%; (k) NaH, MeOH, 75 °C; (l) aq 2M LiOH, MeOH, 60 °C, 18 h, 87%; (m) PyBOP, aminoacetonitrile hydrochloride, Et$_3$N, DMF, 3 h, 82%.

Scheme 2. Synthesis of pyridine N-oxide **5** and pyridones **6** and **7**. Reagents and conditions: (a) NaH, MeOH, 80 °C, 3 h, 68%; (b) m-CPBA, CH$_2$Cl$_2$, rt, 45 min, 66%; (c) 4-(methylthio)benzeneboronic acid, PdCl$_2$(dppf)·CH$_2$Cl$_2$, aq 2 M Na$_2$CO$_3$, DMF, 85 °C, 18 h, 89%; (d) aq 2M LiOH, 75 °C, 18 h, 93%; (e) PyBOP, aminoacetonitrile hydrochloride, Et$_3$N, DMF, 18 h, 44%; (f) TFAA, Et$_3$N, THF, 0 °C → rt, 2 h, 100%; (g) same conditions as (d), 95%; (h) same conditions as (e), 4% for **6** and 6% for **7**.

Scheme 3. Synthesis of the pyrazole analog **10**. Reagents and conditions: (a) malonic acid, pyrrolidine, pyridine, 100 °C, 2 h, 97%; (b) Butadiene, MePh, 200 °C, stainless steel bomb, 24 h, 90%; (c) I$_2$, KI, NaHCO$_3$, CH$_2$Cl$_2$/H$_2$O, 0 °C → rt, 18 h, 59%; (d) Bu$_3$SnH, AIBN, PhH, 80 °C, 1.5 h, 92%; (e) MeONa, MeOH, 0 °C → rt, 18 h, 96%; (f) Jones' oxidation, Me$_2$CO, 0 °C → rt, 0.5 h, 85%; (g) DAST, CH$_2$Cl$_2$, 0 °C → rt, 2 h, 38% (26% alkenes + 12% SM); (h) 4-(methylthio)benzeneboronic acid, PdCl$_2$(dppf)·CH$_2$Cl$_2$, aq. 2M Na$_2$CO$_3$, DMF, 90 °C, 3 h, 33%; (i) aq 2M LiOH, THF/MeOH (2:1), rt, 18 h, 100%; (j) aminoacetonitrile hydrochloride, HATU; i-Pr$_2$NEt, DMF, rt, 18 h, 96%.

200 °C afforded the desired cycloadduct **26** in good yield (90%). Iodolactonization yielded **27** which was de-iodinated under radical conditions to afford the bicyclic lactone **28**. Cleavage of the lactone **28** with NaOMe provided **29** which was oxidized with Jone's reagent and difluorinated using DAST to afford compound **30**. Suzuki cross-coupling of heteroaryl bromide **30** with 4-methyl-thiobenzeneboronic acid yielded compound **31** which was hydrolyzed to the corresponding carboxylic acid **32** and coupled with aminoacetonitrile to afford the final compound **10**.

All other reported compounds were prepared analogously, using either of the two routes shown above, with minor modifications.

In this report, we have disclosed further SAR demonstrating that the P2–P3 1,2-disubstituted phenyl linker of **1** can be replaced with various 5- and 6-membered heteroaromatic rings. This approach was first based on the rationale that the P2–P3 phenyl linker is solvent-exposed in the inhibitor–enzyme complex and that the incorporation of polarity in this region of our lipophilic inhibitors would be tolerated and could potentially decrease the magnitude of the shift observed in the bone resorption functional assay. While inhibitors in the pyridine/pyridone series succeeded in decreasing this shift, none of these achieved the sub-nanomolar potency of our lead compound (±)-**1**.

Second, it was hypothesized that replacing the 6-membered ring with a 5-membered ring would allow for tighter binding of the inhibitor with the active site and potentially improve potency. This strategy enabled us to identify the thiazole analog **9** (IC$_{50}$ = 0.2 nM) that showed superior potency over our lead inhibitor (±)-**1** (IC$_{50}$ = 0.5 nM). While the 5-membered heteroaromatic inhibitors were still highly shifted in the functional

assay, the potent and selective pyrazole analog **10** displayed an improved pharmacokinetic profile over our lead compound (−)-**1**. Based on our findings we are currently exploring strategies to incorporate additional polarity into the 5-membered heteroaromatic-linked series, and identify a cyclohexanecarboxamide based Cat K inhibitor that exhibits an acceptable shift ($\leqslant$10-fold) in our functional assay. The results of these investigations will be reported in due course.

References and notes

1. (a) Bromme, D.; Okamoto, K.; Wang, B. B.; Biroc, S. *J. Biol. Chem.* **1996**, *271*, 2126; (b) Bossard, M. J.; Tomaszek, T. A.; Thompson, S. K.; Amegadzie, B. Y.; Hanning, C. R.; Jones, C.; Kurdyla, J. T.; McNully, D. E.; Drake, F. H.; Gowen, M.; Levy, M. A. *J. Biol. Chem.* **1996**, *271*, 12517; (c) Tezuka, K.; Tezuka, Y.; Maejima, A.; Sato, T.; Nemoto, K.; Kamioka, H.; Hakeda, Y.; Kumegawa, M. *J. Biol. Chem.* **1994**, *269*, 1106; (d) Turk, B.; Turk, D.; Turk, V. *Biochim. Biophys. Acta* **2000**, *1477*, 98; (e) Drake, F. H.; Dodds, R. A.; James, I. E.; Connor, J. R.; Debouk, C.; Richardson, S.; Lee-Rykaczewski, E.; Coleman, L.; Rieman, D.; Barthlow, R.; Hastings, G.; Gowen, M. *J. Biol. Chem.* **1996**, *271*, 12511; (f) Troen, B. R. *Drug News Perspect.* **2004**, *17*, 19.
2. (a) Peck, W. A.; Burckhardt, P.; Christiansen, C.; Fleisch, H. A.; Genant, H. K.; Gennari, C.; Martin, T. J.; Martini, L.; Morita, R.; Ogata, E.; Rapado, A.; Shulman, L. E.; Stern, P. H.; Young, R. T. T.; Barrett-Connor, E.; Brandi, M. L.; Chestnut, C. H.; Delmas, P. D.; Heaney, R. P.; Johnston, C. C.; Kanis, J. A.; Lindsay, R.; Meunier, P. J.; Papapoulous, S. E.; Reginster, J. Y.; Riggs, B. L.; Riis, B. J.; Seeman, E.; Wasnich, R. D. *Am. J. Med.* **1993**, *94*, 646; (b) Blair, H. C.; Athanasou, N. A. *Histol. Histopathol.* **2004**, *19*, 189.
3. (a) Black, W. C.; Bayly, C. I.; Davis, D. I.; Desmarais, S.; Falgueyret, J.-P.; Léger, S.; Li, C. S.; Massé, F.; McKay, D. J.; Palmer, J. T.; Percival, M. D.; Robichaud, J.; Tsou, N.; Zamboni, R. *Bioorg. Med. Chem. Lett.* **2005**, *15*, 4741; (b) Li, C. S. ; Deschenes, D.; Desmarais, S.; Falgueyret, J.-P.; Gauthier, J. Y.; Kimmel, D. B.; Léger, S.; Massé, F.; McKay, D. Percival, M. D.; Riendeau, D.; Rodan, S. B.; Somoza, J.; Thérien, M.; Truong, V. -L.; Wesolowski, G.; Zamboni, R.; Black, W. C. *Bioorg. Med. Chem. Lett.* **200**, *15*, 4741; (c) Robichaud, J.; Bayly, C.; Oballa, R.; Prasit, P.; Mellon, C.; Falgueret, J.-P.; Percival, M. D.; Wesolowski, G.; Rodan, S. B. *Bioorg. Med. Chem. Lett.* **2004**, *14*, 4291; (d) Robichaud, J.; Oballa, R.; Prasit, P.; Falgueyret, J.-P.; Percival, M. D.; Wesolowski, G.; Rodan, S.; Kimmel, D.; Johnson, C.; Bryant, C.; Venkatraman, S.; Setti, E.; Mendoca, R.; Palmer, J. *J. Med. Chem.* **2003**, *46*, 3709.
4. Crane, S. N.; Black, W. C.; Palmer, J. T.; Davis, D. E.; Setti, E.; Robichaud, J.; Paquet, J.; Oballa, R. M.; Bayly, C. I.; McKay, D. J.; Somoza, J. R.; Chauret, N.; Seto, C.; Scheigetz, J.; Wesolowski, G.; Massé, F.; Desmarais, S.; Ouellet, M. *J. Med. Chem.* **2006**, *49*, 1066.
5. Falgueyret, J.-P.; Black, W. C.; Cromlish, W.; Desmarais, S.; Lamontagne, S.; Mellon, C.; Riendeau, D.; Rodan, S.; Tawa, P.; Wesolowski, G.; Bass, K. E.; Venkatraman, S.; Percival, D. *Anal. Biochem.* **2004**, *335*, 218.
6. Falgueyret, J.-P.; Oballa, R. M.; Okamoto, O.; Wesolowski, G.; Aubin, Y.; Rydzewski, R. M.; Prasit, P.; Riendeau, D.; Rodan, S. B.; Percival, M. D. *J. Med. Chem.* **2001**, *44*, 94.
7. Small amounts of the isomeric fluoroalkenes were produced along with **18** but were removed via chromatography in the subsequent steps.